EFFECTS OF MAGMA OCEAN CRYSTALLIZATION ON THE LONG-TERM THERMOCHEMICAL EVOLUTION OF THE MOON I. Bernt[1], A.-C. Plesa[1], S. Schwinger[1], M. Collinet[1], D. Breuer[1], [1]German Aerospace Center (DLR), Rutherfordstr. 2, 12489 Berlin (irene.bernt@dlr.de) .

Introduction: The early stages of lunar evolution have been characterized by the existence of a magma ocean. Fractional crystallization of the latter resulted in an inhomogeneous mantle with cumulate layers of increasing density towards the surface, due to iron enrichment in the residual magma ocean [1]. Such an unstable density distribution is prone to overturn and sets the stage for the subsequent thermochemical history of the mantle. In particular, this initial stage can significantly affect mixing of mantle material and the partial melt production, as well as the melt composition during the later stages of lunar evolution. The melt composition is directly linked to the composition of lunar basalts, whose variability at the lunar surface indicates complex melting processes and the presence of various mantle reservoirs.

In this study we model the solid-state convection, mixing, and partial melt production in the lunar mantle. We investigate the effects of an initially layered mantle as a consequence of the fractional crystallization of the lunar magma ocean and compare it to an initially homogeneous mantle, as it was used in many previous studies. While previous mantle convection studies investigated lunar mantle melting in a purely homogeneous mantle [2] or with a localized KREEP layer [3], here we combine petrological and geodynamical models to investigate the degree of heterogeneity that can be produced by melting and mixing of an initially heterogeneous lunar mantle. In addition, we constrain possible model parameters for both homogeneous and heterogeneous mantle scenarii using the estimated secondary crustal thickness of the Moon.

Petrological Model: *Heterogeneous lunar mantle compostion case:* The petrological model computes the crystallization sequence of the lunar magma ocean (LMO) in the heterogeneous case. For the calculations we follow the approach described by [4], which is in good agreement with experimental data [5, 6] for the whole solidification process. We assume fractional crystallization of a spherical shell with an initial LMO thickness of 1350 km and a bulk lunar mantle composition from [7].

The resulting mantle structure is characterized by 5 compositional layers, where the predominant minerals are olivine, orthopyroxene, clinopyroxene, clinopyroxene and ilmenite (ilmenite bearing cumulates = IBC) and plagioclase (crust), respectively. For each of these layers an average density is calculated at the end of the crystallization sequence, as well as the change in density as a function of mantle depletion due to melting. The solidus and liquidus temperature profiles are calculated for the average compositions in each layer using alphaMELTS.

The results from the petrological model are shown in Fig. 1. The densities of the mantle layers increase with radius due to the enrichment of iron in the remaining melt during crystallization. The crust has a comparative low density (Fig. 1a). The temperature profile follows the crystallization temperatures of the cumulates. In Fig. 1c, the temperature profile is shown together with the individual layers and their corresponding solidi.

Homogeneous lunar mantle composition case: For the homogeneous case we use a KLB-1 peridotite [8] mantle composition, for which the solidus and liquidus, as well as the density-update due to mantle depletion were calculated using alphaMELTS. The initial temperature profile follows the approach used in [3], and is shown in Fig. 1b).

Geodynamical Model: We use the mantle convection code GAIA [9] in a 2D quarter cylinder geometry to model the thermochemical evolution of the compositionally homogeneous or heterogeneous lunar mantle. We employ an Arrhenius law to calculate the temperature- and depth-dependent viscosity. To track the composition of the mantle we use a particle-in-cell (PIC) method [10], where tracer particles carry information about material properties such as density, melting temperature, degree of depletion, amount of heat producing elements etc. In our simulations we account for core cooling and radioactive decay, as well as mechanical mixing. In addition, we consider the effects of melting by accounting for the latent heat during mantle melting, as well as solidus increase and density decrease due to mantle depletion [11].

Results: We use estimates of the average thickness of the basaltic crust that was formed by convection and melting processes during the lunar evolution after the crystallization of the LMO. These estimates show large uncertainties and vary from roughly 2 to 5 km [12]. Here we use a conservative range of 2 to 10 km, since basaltic melt may remain trapped in the lithosphere in form of intrusive melt. *Homogeneous case:* The initial temperature profile has a significant impact on the amount of melt produced in the homogeneous case. Previous studies found that even intermediate temperature profiles produce rather large amounts of secondary crust [3]. Our models indicate that to produce a secondary basaltic crust of thickness consistent with current estimates (max. 10 km) a relatively cold

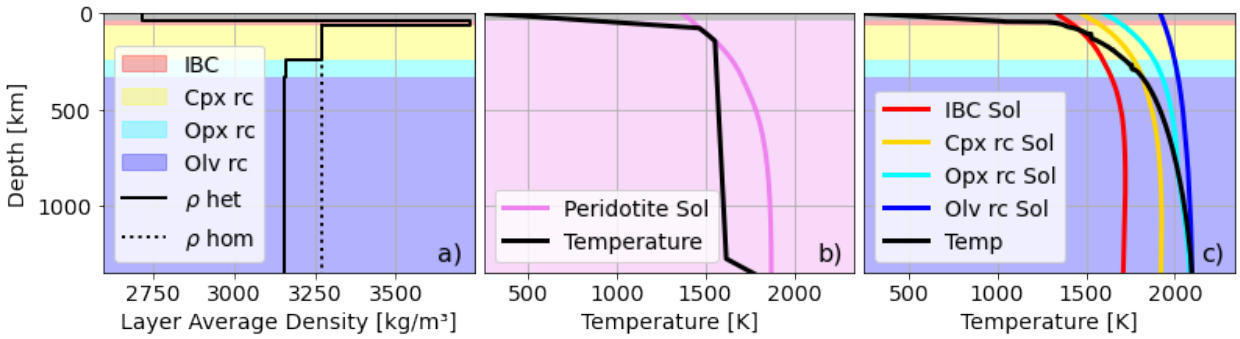

Figure 1: Initial input for the geodynamical model, generated by the petrological model. a) The density profiles for both scenarii (initial homogeneous and initial heterogeneous mantle) together with the initial layers in the heterogeneous case. b) Initial temperature profile and solidus of the peridotite mantle in the homogeneous case. c) Initial temperature profile and solidi of the heterogeneous mantle composition case. (rc = rich cumulates, het = heterogeneous case, hom = homogeneous case, Sol = solidus, ρ= density)

initial potential mantle temperature of 1506–1555 K is required. This temperature profile (Fig. 1b) would imply an abnormally small initial magma ocean depth of only 106–145 km. In addition, such low initial temperatures lead to a delayed secondary crust production (Fig. 2).

Heterogeneous case: In contrast to the homogeneous case, the initial temperature profile of the heterogeneous case is given by the solidification temperature (Fig. 1c). One important aspect in this case is the stability of the IBC layer. Sinking of the IBC cumulates influences the interior dynamics of the lunar mantle and the amount of melt produced. If the IBC layer remains trapped in the stagnant lid, the models show an average thickness of 1.3 km of basaltic crust produced during the evolution. On the other hand, if about 35% of the IBC sinks into the mantle it leads to an average thickness of the basaltic crust of 2 km. The higher amount of melt produced in this case results from the fact that sinking

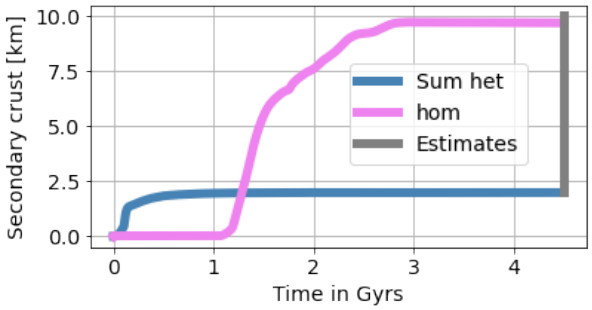

Figure 2: Comparison of the crustal thicknesses for a heterogeneous case with a homogeneous case. The initial temperature profile for the homogeneous case has a potential temperature of 1555 K, corresponding to an initial magma ocean depth of 145 km. In the heterogeneous case about 35% of the IBC layer sinks into the mantle. The acceptable crustal thickness range is shown by the grey vertical line.

of the IBC cumulates lead to a stronger return flow that promotes mantle melting and due to melting of IBC cumulates themselves, which have the lowest melting temperature of all mantle components.

Conclusion: With our coupled petrological-geodynamical model we are able to constrain thermal evolution parameters of an initially homogeneous and an initially heterogeneous lunar mantle. Using the secondary crustal thickness as a constraint, we find that a heterogeneous mantle composition yields more comparable results to observational estimates than a homogeneous mantle composition. In the latter case only a cold initial temperature profile would be compatible with a basaltic crustal thickness as suggested by observations. In an initially heterogeneous mantle, at least parts of the IBC layer need to be recycled into the mantle to obtain a secondary crustal thickness in the range of the inferred basaltic crust estimates. In future work we will compare the melt composition obtained in our calculations to the observed composition of mare basalts to include additional constraints for our models. Furthermore, we plan to investigate convection and mixing of the cumulates during the LMO crystallization.

Acknowledgements: We thank Brian Doherty for his contribution to the numerical implementation. I.B. and S.S. were supported by the German Research Foundation (Deutsche Forschungsgemeinschaft) SFB-TRR170, (subprojects C4 and A5).

References: [1] Elkins-Tanton L.T. (2012) *Annu. Rev. Earth Planet. Scie.* [2] Ziethe R. et al. (2009) *P&SS*; [3] Laneuville M. et al. (2013) *JGR: Planets*; [4] Schwinger S. and Breuer D. (2021) *PEPI*; [5] Rapp J.F. and Draper D.S. (2018) *MAPS*; [6] Charlier B. et al. (2018) *Geochim. Cos- mochim. Acta*; [7] O'Neill H.St.C. (1991) *Geochim. Cosmochim. Acta*; [8] Zhang J. and Herzberg C. (1994) *JGR: Solid Earth*; [9] Hüttig C. et al. (2013) *PEPI*; [10] Plesa A.C. et al. (2013) *IGI Global*; [11] Breuer D. et al. (2018) *AGU Fall Meeting*; [12] Shengxia G. et al. (2016) *JGR: Planets*.